APPENDIX

Stable kinetochore-microtubule attachment requires loop-dependent Ndc80-Ndc80 binding

Soumitra Polley[1], Helen Müschenborn[1,a], Melina Terbeck[1], Anna De Antoni[2,b], Ingrid R. Vetter[1], Marileen Dogterom[3], Andrea Musacchio[1,4*], Vladimir A. Volkov[3,5*], Pim J. Huis in 't Veld[1*]

Table of Contents Page

Appendix Figure S1 Preparation of full-length and loopless Ndc80, TS[Ndc80]$_3$ modules and coated beads.

A) The fluorescent peptide, Sortase, and labelled Ndc80 complexes with (full-length, blue) and without (Δloop, orange) the loop were separated using size-exclusion chromatography. The gray area indicates Ndc80 that was collected and (without further concentration) stored for further use.

B) Ndc80 complexes from panel A were analysed by in-gel fluorescence and Coomassie staining following SDS-PAGE. These complexes were used for experiments shown in **Figure 1F-K** and **Figure 5A-D**.

C) Full-length and loopless Ndc80 complexes (Sortase labelled with FAM) were analysed by mass photometry. Determined and theoretical masses are indicated in the legend. These complexes were also used for the SEC-MALS shown in **Figure 1D**.

D) Schematic overview of the preparation of Ndc80 trimers. The fluorescent peptide, Sortase, labelled Ndc80 monomers (full-length, blue; Δloop, orange), and Ndc80 trimers were separated using size-exclusion chromatography. Selected fractions containing Ndc80 trimers are marked in grey and were analysed by SDS-PAGE. Since samples were not boiled, the streptavidin scaffold and the covalently bound SPC24 subunits remain intact. See the Materials and Methods and (Volkov et al., 2018) for more information.

E) Brightness of PLL-PEG-conjugated beads with various percentage of biotinylation, subsequently saturated with Ndc80^{TMR} trimers. Shown are mean and SD. Each datapoint represents a single bead preparation, at least 50 beads were quantified for each preparation.

F) Fraction of stalls resulting in a rescue, binned by individual bead preparation, and correlated to the median bean brightness in that preparation.

Appendix Figure S2 Chemical crosslinking followed by mass spectrometry and proximity maps.

A) Crosslinking procedure and SDS-PAGE analysis of Ndc80, Mis12:Ndc80, Ndc80$^{\Delta loop}$, and Mis12:Ndc80$^{\Delta loop}$. The asterisks indicate the four subunits of the Mis12 complex.

B) Analysis of side-chains crosslinked by DSBU in the various samples. M refers to the free NH_2-terminus.

C) Mapping of all (left) and top-scoring (right) crosslinks of full-length Ndc80 on the predicted structure of the full-length Ndc80 complex. A subset of crosslinks, all with a false-discovery rate below 1%, connect residues that are far apart in the extended Ndc80 structure. For instance, SPC25 K133 and K203 connect to various regions of the complex. Whether these long-distance crosslinks reflect transient compacted conformations of Ndc80 or transient inter-complex interactions is unclear. Lengths indicate C_α- C_α distances. Crosslinks spanning a distance below 30 Å are shown separately, with magnifications of the loop and tetramerisation regions.

D) Mapping of all (left) and top-scoring (right) crosslinks of Ndc80$^{\Delta loop}$ on the predicted structure of the full-length Ndc80 complex. Crosslinks spanning a distance below 30 Å are shown separately, with magnifications of the loop and tetramerisation regions, as well as a prediction of the loopless Ndc80 region.

Appendix Figure S3 An NDC80:NUF2 fragment encompassing the loop is monomeric and does not bind Ndc80.

A) Size-exclusion chromatography analysis (Superdex 75 16/600) of the NDC80:NUF2 loop fragment before and after cleavage of the GST-tag. The N-terminus of NDC80$^{376\text{-}517}$ was fluorescently labeled using Sortase following GST cleavage.

B) GST or GST-NDC80:NUF2 was immobilized on beads and incubated with the NDC80:NUF2 fragment, full-length Ndc80, or loopless Ndc80.

Appendix Figure S4 Effects of AB-849 and AB-850 in vitro.

A) A fluorescently labelled secondary antibody was used to exclude microtubule binding of primary antibodies in the absence of Ndc80. Scale bar: 5 µm.

B) The brightness of loopless Ndc80 trimers in absence and in presence of crosslinking antibodies was followed over time. Trimers accumulate in 10 minutes in an antibody depending manner (AB-850 does not recognize loopless Ndc80).

C) Initial brightness distributions of Ndc80 trimers. Shaded areas mark datapoints used to analyse diffusion (**Figure 6**). To enable experiments with antibodies, these experiments were performed without reducing agents.

D) Comparable conditions as in panel C, but with the buffer including reducing reagents that was used for other *in vitro* experiments with microtubules (such as in **Figure 2D-E**).

Appendix Figure S5 Clustering of Ndc80 mutants on microtubules.

A) SDS-PAGE analysis and in-gel fluorescence of eight different FAM-labelled Ndc80 complexes used to analyse Ndc80 clustering on microtubules.

B) The standard deviation (SD) of Ndc80 fluorescence along microtubules was determined as a readout for distribution uniformity. Median, 25-75% boxes, and 5-95% boxes were determined for eight Ndc80 variants. Example micrographs (and their corresponding SD values) are shown.

Appendix Figure S1 - Preparation of full-length and loopless Ndc80,TS[Ndc80]3 modules, and coated beads

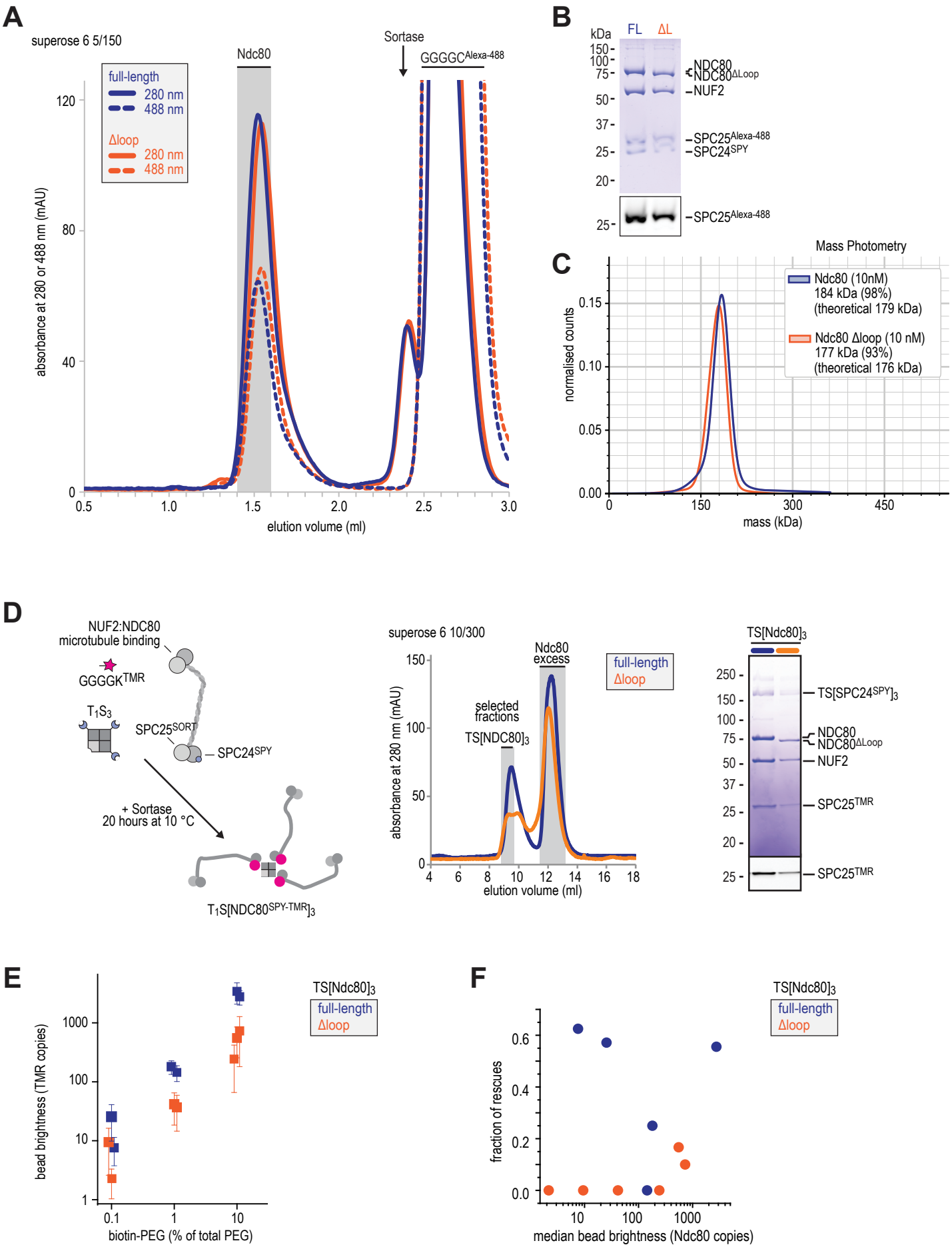

Appendix Figure S2 - Chemical crosslinking followed by mass spectrometry and proximity maps

A

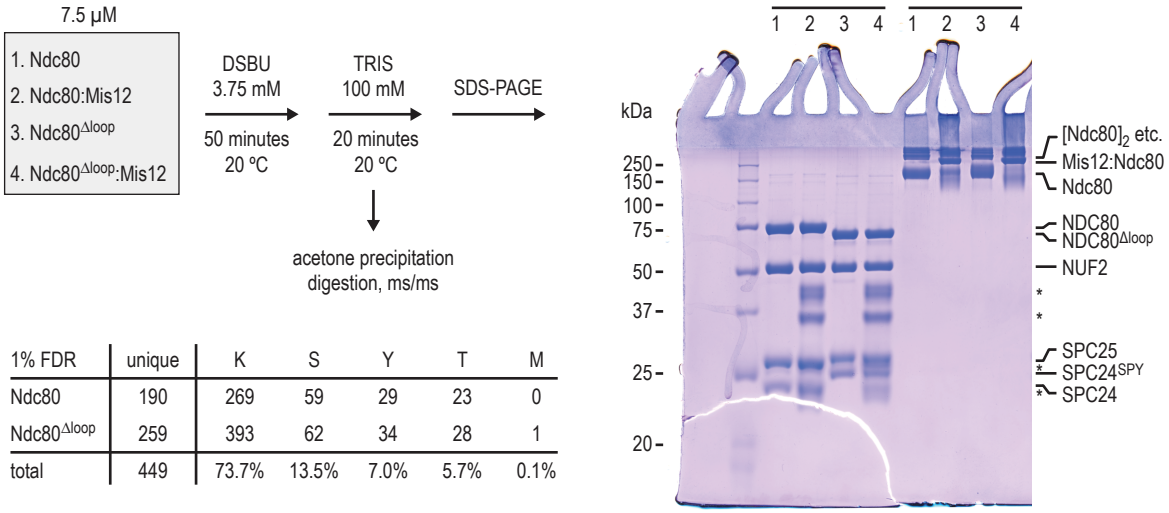

B

1% FDR	unique	K	S	Y	T	M
Ndc80	190	269	59	29	23	0
Ndc80$^{\Delta loop}$	259	393	62	34	28	1
total	449	73.7%	13.5%	7.0%	5.7%	0.1%

C

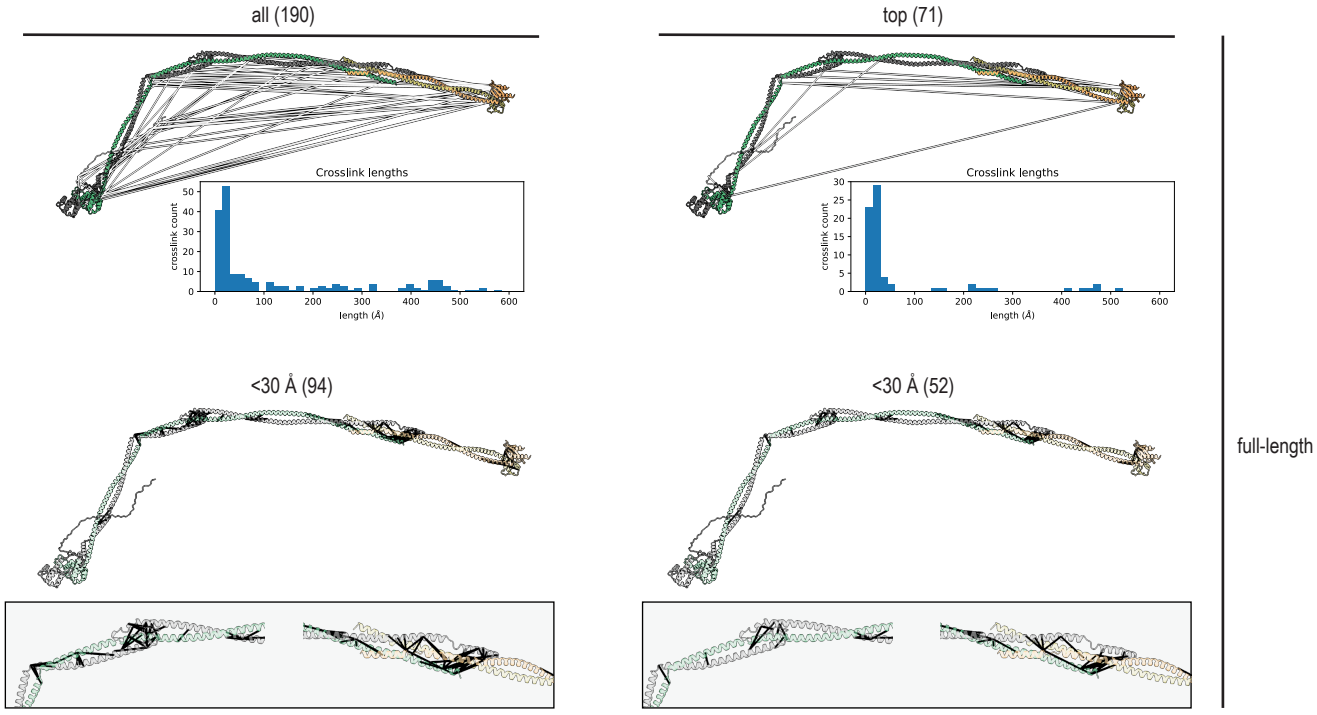

D

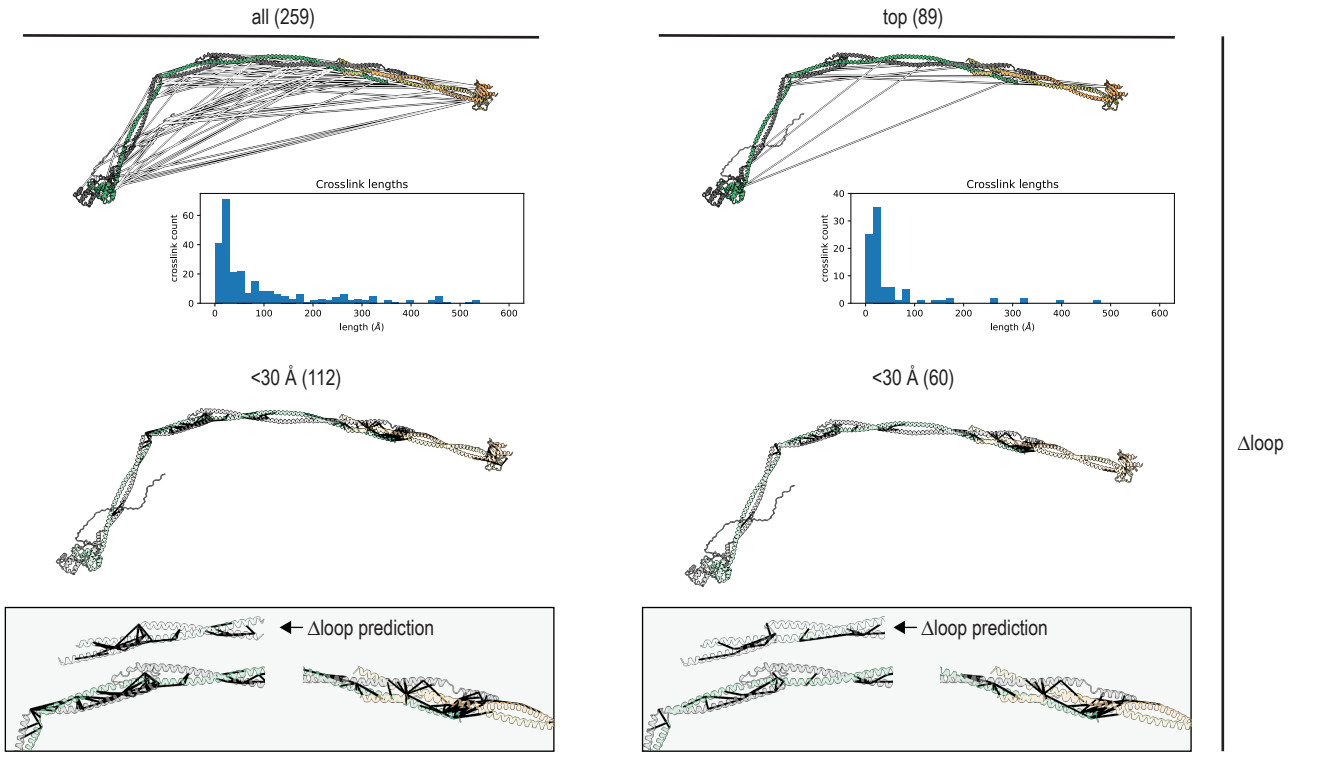

Appendix Figure S3 - An NDC80:NUF2 fragment encompassing the loop is monomeric and does not bind Ndc80

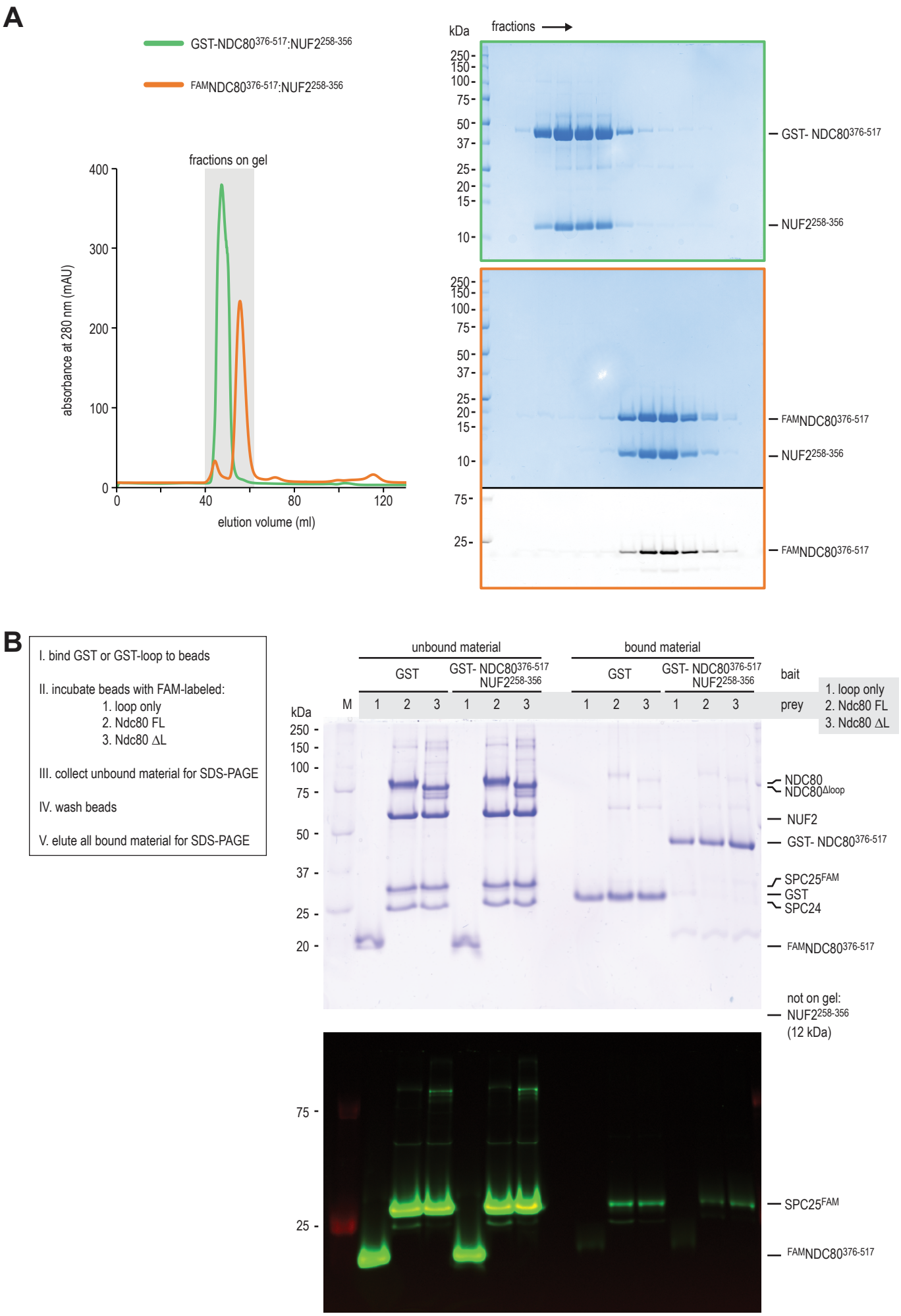

Appendix Figure S4 - Effects of AB-849 and AB-850 in vitro

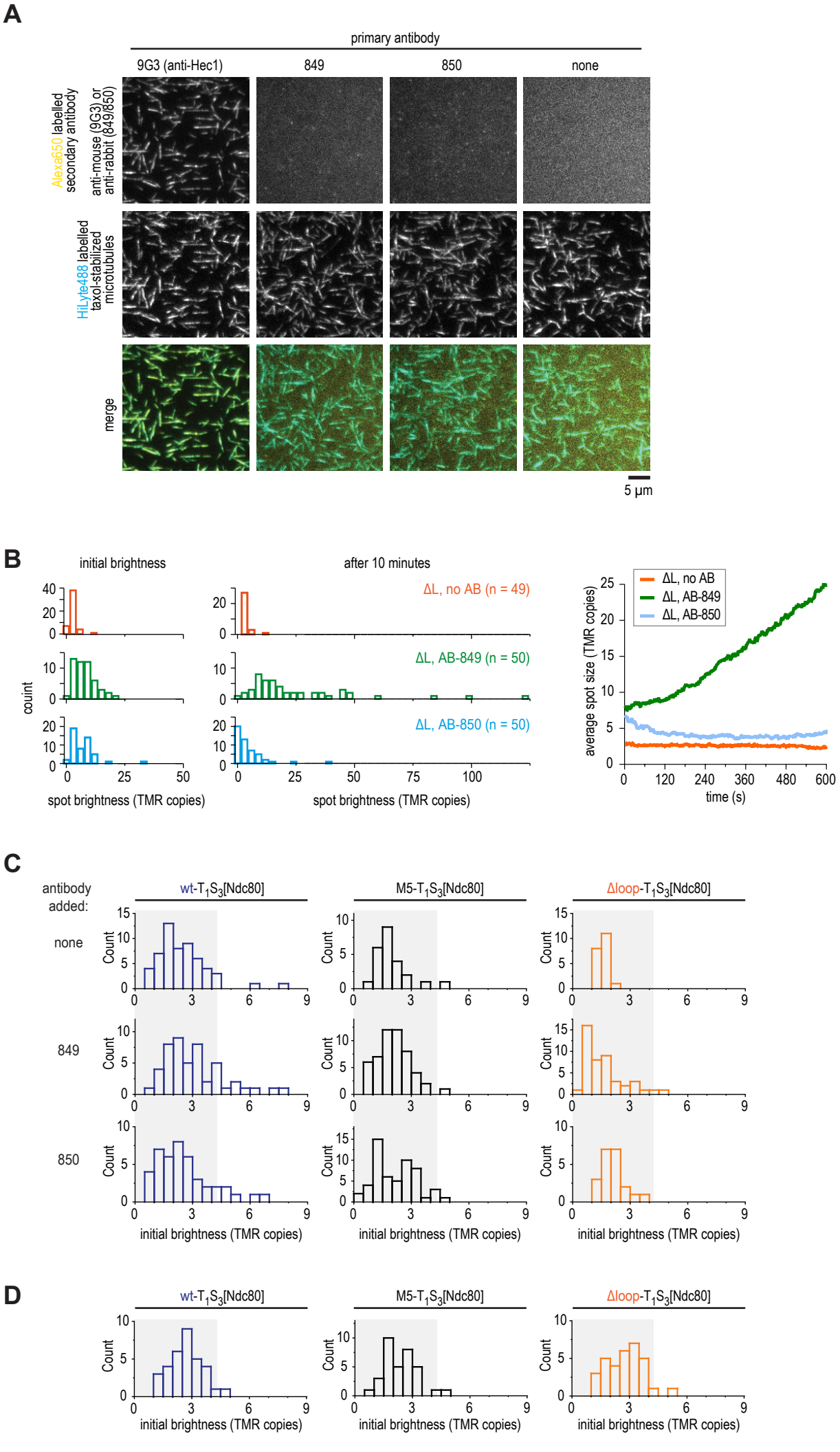

Appendix Figure S5 - Clustering of Ndc80 mutants on microtubules